Original Article

Cystatin C Is Associated with the Extent and Characteristics of Coronary Atherosclerosis in Patients with Preserved Renal Function

(cystatin C / coronary plaque / intravascular ultrasound / virtual histology)

A. KRÁL[1], T. KOVÁRNÍK[1], Z. VANÍČKOVÁ[2], H. SKALICKÁ[1], J. HORÁK[1], K. BAYEROVÁ[1], Z. CHEN[3], A. WAHLE[3], L. ZHANG[3], K. KOPŘIVA[4], H. BENÁKOVÁ[2], M. SONKA[3], A. LINHART[1]

[1]2nd Department of Medicine – Department of Cardiovascular Medicine, [2]Institute of Medical Biochemistry and Laboratory Diagnostics, First Faculty of Medicine, Charles University and General University Hospital in Prague, Czech Republic
[3]Iowa Institute for Biomedical Imaging, Department of Electrical & Computer Engineering, The University of Iowa, Iowa City, IA, USA
[4]Cardiology Department of Homolka Hospital, Prague, Czech Republic

Abstract. Cystatin C (CysC), an endogenous inhibitor of cysteine proteases and a sensitive and accurate marker of renal function, is associated with the severity of coronary atherosclerosis assessed by angiography and future cardiovascular events according to previous studies. We aimed to evaluate the association between CysC levels and coronary plaque volume, composition and phenotype assessed by intravascular ultrasound and intravascular ultrasound-derived virtual histology in patients with preserved renal function. Forty-four patients with angiographically documented coronary artery disease and complete intravascular imaging were included in the study. Patients were categorized into tertiles by CysC levels. Subjects in the high CysC tertile had significantly higher mean plaque burden (48.0 % ± 6.9 vs. 42.8 % ± 7.4, P = 0.029), lower mean lumen area (8.1 mm[2] ± 1.7 vs. 9.9 mm[2] ± 3.1, P = 0.044) and a higher number of 5-mm vessel segments with minimum lumen area < 4 mm[2] (17.9 ± 18.9 vs. 6.8 ± 11.7, P = 0.021) compared to patients in the lower tertiles. In addition, CysC levels demonstrated significant positive correlation with the mean plaque burden (r = 0.35, P = 0.021). Neither relative, nor absolute plaque components differed significantly according to CysC tertiles. The Liverpool Active Plaque Score was significantly higher in the high CysC tertile patients (0.91 ± 1.0 vs. 0.18 ± 0.92, P = 0.02). In conclusion, our study demonstrated a significant association of increased CysC levels with more advanced coronary artery disease and higher risk plaque phenotype in patients with preserved renal function.

Abbreviations: CABG – coronary artery bypass grafting, CAD – coronary artery disease, CAG – coronary angiography, CD40L – cluster of differentiation 40 ligand, CSA – cross-sectional area, CysC – cystatin C, DES – drug-eluting stents, EEM – external elastic membrane, eGFR – estimated GFR, GFR – glomerular filtration rate, hs-CRP – high-sensitivity C-reactive protein, ICAM-1 – intercellular adhesion molecule 1, IL-1 β – interleukin lβ, IL-6 – interleukin 6, IFN-γ – interferon γ, IVUS – intravascular ultrasound, LAPS – Liverpool Active Plaque Score, MDRD – modification of diet in renal disease, MLA – minimal lumen area, MMP – matrix metalloproteinase, PB – plaque burden, PCI – percutaneous coronary intervention, PRS – plaque risk score, SCr – serum creatinine, TCFA – thin cap fibroatheroma, ThCFA – thick cap fibroatheroma, TNF-α – tumour necrosis factor α, VCAM-1 – vascular cell adhesion molecule 1, VH – virtual histology, VSMC – vascular smooth muscle cells.

Introduction

The atherosclerotic process involves substantial remodelling of the arterial extracellular matrix. In addition to serine proteases and matrix metalloproteinases (MMP), the cysteine proteases cathepsins and their competitive inhibitors cystatins serve an important role in the degradation of extracellular matrix components,

chiefly collagen and elastin, and vascular wall remodelling (Sukhova et al., 2005; Cheng et al., 2011; Salgado et al., 2013). Cystatin C (CysC), the most abundant member of the cystatin superfamily of cysteine protease inhibitors, is a low-molecular-weight protein (13.4 kDa) consisting of 120 amino acids, synthesized in all nucleated cells. In addition to its protease inhibitory function, CysC also acts as an immunomodulatory molecule by decreasing the sensitivity of macrophages to interferon γ (IFN-γ) stimulation (Frendéus et al., 2009). Furthermore, CysC induces NO production by up-regulating inducible nitric oxide synthase (iNOS) in macrophages (Verdot et al., 1999). Recent findings suggest that CysC is regulated by multiple mechanisms at the transcriptional, as well as post-translational level (Xu et al., 2015). Importantly, cystatins are regulated by pro-inflammatory cytokines and growth factors, e.g., transforming growth factor β1 (TGF-ß1) and IFN-γ (Shi et al., 1999; Eriksson et al., 2004).

Human atherosclerotic plaques display increased expression of cathepsins S and K compared with normal vessels. It has been demonstrated that human vascular smooth muscle cell (VSMC) and endothelial cell cathepsin-dependent proteolytic activity is induced by pro-inflammatory cytokines, e.g. tumour necrosis factor α (TNF-α), interleukin l ß (IL-1β), IFN-γ and growth factors (Sukhova et al., 1998, 2005). Conversely, human atherosclerotic lesions show reduced CysC levels compared with normal arteries (Shi et al., 1999). Data from murine experiments further support the role of CysC in the pathogenesis of atherosclerosis. In one study, CysC and apolipoprotein E-deficient (cysC-/- apoE-/-) mice fed an atherogenic diet developed significantly larger subvalvular aortic plaques characterized by increased total macrophage content compared with cysC+/+ apoE-/- mice, suggesting an atheroprotective role of CysC (Bengtsson et al., 2005). Another group using the same experimental animals (CysC-/- apoE-/- mice) found that CysC-deficient mice exhibited significantly increased elastic lamina fragmentation of the tunica media, decreased medial size, and dilatation of the thoracic and abdominal aorta compared with control mice, implying that CysC crucially participates in the regulation of media elastic laminae integrity (Sukhova et al., 2005). Furthermore, CysC-deficient VSMCs exhibited higher cathepsin L and S activity upon pro-inflammatory cytokine and growth factor stimulation in this study (Sukhova et al., 2005). In summary, current observations indicate that an imbalance between tissue levels of cysteine proteases and their inhibitors might play an important role in human atherosclerosis.

CysC is freely filtered in the glomerulus, then reabsorbed and fully degraded in the proximal tubular cells. In recent years, CysC has been proposed as a sensitive and accurate marker of renal function, less affected by age, race, gender, muscle mass and diet than serum creatinine, serving as an alternative parameter for glomerular filtration rate (GFR) estimation (Stevens et al., 2006). In contrast to the observed reduced tissue levels of CysC

in human atherosclerotic lesions, numerous studies have shown increased serum CysC levels to be predictive of future cardiovascular events in patients with acute coronary syndromes (Silva et al., 2012), stable coronary artery disease (Ix et al., 2007), patients after elective percutaneous coronary intervention (PCI) with drug-eluting stents (DES) (Sai et al., 2016), as well as in the general elderly population (Shlipak et al., 2005). Furthermore, several studies in individuals with preserved renal function (i.e., GFR > 60 ml/min) have demonstrated an association of CysC with the presence and severity of coronary artery disease (CAD) assessed by means of coronary angiography (CAG) (Niccoli et al., 2008; Kiyosue et al., 2010; Wang et al., 2014).

Thus, CysC has been proposed as a novel marker for CAD prediction and risk stratification in individuals without renal dysfunction (Koc et al., 2010). Different intravascular imaging modalities including intravascular ultrasound (IVUS) and IVUS-derived virtual histology (IVUS-VH) are utilized for precise characterization of coronary artery atherosclerotic disease. IVUS and IVUS-VH-derived parameters, e.g. plaque burden and composition, provide significant incremental prognostic value compared to CAG (Stone et al., 2011; Hong et al., 2013). However, sparse data exist on the relationship of CysC and coronary plaque magnitude and composition assessed by intravascular imaging (Gu et al., 2009). In this study, we aimed to evaluate the association between CysC levels and coronary plaque volume, composition, and phenotype assessed by IVUS and IVUS-VH and the correlation of CysC levels with inflammatory markers in patients with preserved renal function.

Material and Methods

Patient population

We used data from baseline examinations of 44 patients included in the trial "*The prediction of extent and risk profile of coronary atherosclerosis and their changes during lipid-lowering therapy based on non-invasive techniques*", NCT01773512. In brief, this trial enrolled patients with stable angina and preserved renal function (eGFR > 60 ml/min/1.73 m^2 according to the MDRD formula) who were indicated for CAG due to symptoms. All subjects provided informed consent. The study protocol conforms to the ethical guidelines of the 1975 Declaration of Helsinki as reflected in a priori approval by the institution's human research committee. The study was approved by the institutional review boards of the General University Hospital, Prague, Czech Republic.

Intravascular ultrasound and virtual histology

We analysed 44 baseline datasets that met the following criteria:
1) IVUS-VH of a native coronary artery with stenosis ≤ 50 % of lumen diameter determined by angiography with no indication for either PCI or coronary artery bypass grafting (CABG) at the time of initial imaging;

2) Good-quality IVUS-VH pullbacks (i.e., without noticeable pullback speed discontinuity);

3) Imaged vessels free of severe calcification to avoid inconsistency of IVUS-VH plaque type determination in areas of acoustic shadowing;

4) Examined segments at least 30 mm long with plaque burden (PB) > 20 %.

One segment of a coronary artery from each patient was chosen for the study. The lesion located in the proximal coronary segment or located in non-angulated segment was selected if several similar stenoses were present in the imaged vessel.

IVUS was performed in the standard fashion using the IVUS phased-array probe (Eagle Eye 20 MHz 2.9F monorail, Volcano Corporation, Rancho Cordova, CA), IVUS console, Gold standard software, with automatic pullback at 0.5 mm/s (research pullback, model R-l00, Volcano Corporation). After administration of 200 μg of intracoronary nitroglycerin, the IVUS catheter was inserted into the target vessel beyond a distal fiduciary point and then pulled back to the aorto-ostial junction.

Original B-mode IVUS pullback image data were transferred to the Iowa Institute for Biomedical Imaging (Iowa City, IA) for quantitative analysis. For each frame of all IVUS pullbacks, luminal and external elastic membrane (EEM) surfaces were automatically segmented using the fully three-dimensional LOGISMOS graph-based approach (Li et al., 2006; Yin et al., 2010). Automatically determined borders were reviewed and algorithmically refined by an expert reader (TK) using an operator-guided computer-aided interface (Sun et al., 2013). EEM and lumen surfaces/contours served as the input for off-line virtual histology computation using

Volcano's research software, which allows VH computations based on user-supplied segmentation of lumen and external elastic membrane. Employing our previously reported approach (Wahle et al., 1999), geometrically correct fully 3D representation of the vascular wall surfaces and IVUS-VH defined tissue characterization was obtained via fusion of bi-plane angiography and IVUS-VH.

This 3D model served as a basis for quantitative morphologic analyses and quantitative assessment of plaque composition in every frame of the imaged vessel (Wahle et al., 2006). Frame-based indices of plaque morphology and virtual histology were computed and averaged in 5-mm vessel segments. Vessel and plaque measurement morphologic indices included: EEM cross-sectional area (CSA), lumen CSA, PB (EEM CSA – lumen CSA/ EEM CSA) and eccentricity index (max. plaque thickness – min. plaque thickness)/max. plaque thickness) (Mintz et al., 2001, 2011; Nair et al., 2002), (Fig. 1).

Plaque phenotype definitions and plaque scoring systems

VH-IVUS classifies plaques into four tissue types: *fibrous* – F, *fibro-fatty* – FF, *dense calcification* – DC, and *necrotic core* – NC. The plaque composition was expressed both as a relative amount of the four plaque components in percentages as well as their absolute amount in pixels. Using quantitative assessment of virtual histology tissue types, each 5-mm vessel segment was classified into one of six phenotypic categories as previously reported (Garcia-Garcia et al., 2009; Stone et al., 2011):

1) no lesion – NL (plaque burden less than 40 %)
2) pathologic intimal thickening – PIT
3) fibrous plaque – FP
4) fibro-calcific plaque – FcP
5) thick cap fibroatheroma – ThCFA
6) thin cap fibroatheroma – TCFA

based on previously accepted definitions, as per Fig. 2. To determine the TCFA category, three consecutive frames were analysed. Assigning one of the six phenotype category labels to each 5-mm segment was based on the morphologic analysis of each frame within the 5-mm segment – the segment-specific category for each 5-mm segment resulted from the most severe frame-category type within the segment.

In addition to the standard plaque phenotype definitions, we developed a novel plaque stage scoring system, the plaque risk score (PRS), based on the combined weight of plaque phenotype presence in individual IVUS frames by assigning the following weights: TCFA (5 points), ThCFA (4 points), FcP (3 points), FP (2 points), PIT (1 point), NL (0 point). The PRS was calculated for all frames and the highest score within each 5-mm segment determined the risk score for that segment. We also calculated the Liverpool Active Plaque Score (LAPS) to compare this phenotype classification with a previously established plaque scoring
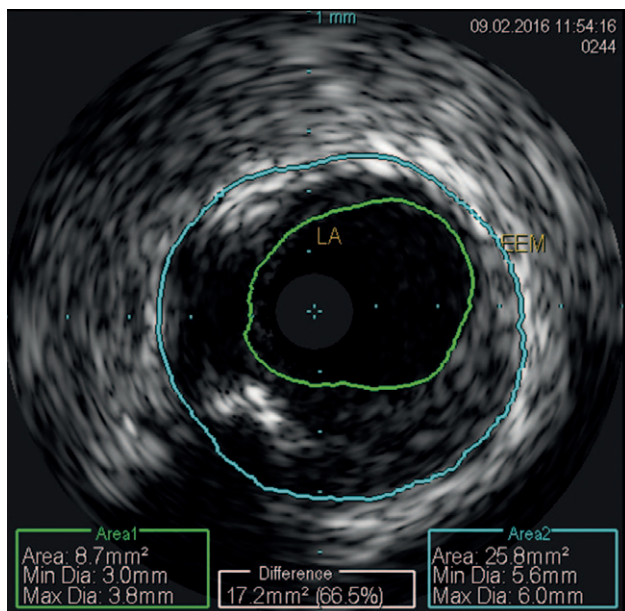

Fig. 1. Plaque burden calculation
Illustration of plaque burden calculation according to the following formula: PB = EEM area – LA/EEM area (in %)
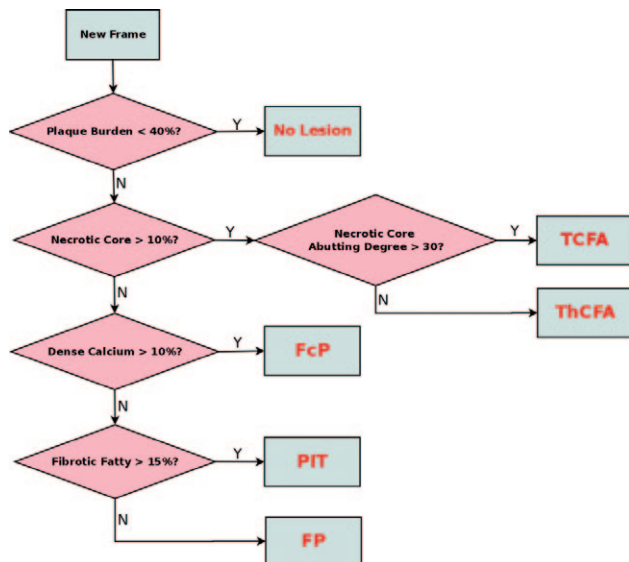LA – lumen area; EEM – external elastic membrane; PB – plaque burden

Fig. 2. Coronary plaque phenotypic categories
Using quantitative assessment of virtual histology tissue types, each 5-mm vessel segment was classified into one of six phenotypic categories:
PIT – pathologic intimal thickening; FP – fibrous plaque; FcP – fibro-calcific plaque; ThCFA – thick cap fibroatheroma; TCFA – thin cap fibroatheroma.

system. We used the following formula: $-2.149 + 0.68 \times$ NC/DC $+ 3.39 \times$ MLA (minimal lumen area) $+ 5.1$ (if remodelling index was > 1.05) $+ 3.7 \times$ TCFA adapted from Murray et al. (2014). The standard LAPS definition was modified solely to account for differences in remodelling definition, as our serial analysis allowed more accurate determination of remodelling based on temporal changes in reference EEM measurements.

Laboratory methods

Samples were centrifuged and aliquoted on the day of venopuncture and stored at -20 °C until analysis. CysC was determined by the latex enhanced turbidimetric method by Diazyme (Powray, CA) in a DxC analyser (Beckman Coulter, Prague, Czech Republic). The method uses anti-human CysC chicken polyclonal antibodies and a 6-point calibration curve. ICAM-1 and VCAM-1 were determined by the ELISA method (eBioscience, Vienna, Austria) with a 6-point calibration curve. CD40L, TNF-α and IL-6 were determined by the ELISA method (RayBiotech, Inc., Norcross, GA) with an 8-point calibration curve. ELISA methods use human-specific antibodies, tetra-methyl benzidine as a substrate, results are read at wavelengths 450 nm with reference wavelengths 570 nm in microplate reader Spectra (SLT-Labinstruments, Salzburg, Austria) and evaluated by KIMW Software (Dan Kittrich, Prague, Czech Republic). TNF-α levels < 1 pg/ml have higher noise-to-signal ratio, and therefore were classified as 0 pg/ml.

GFR estimation was performed according to the simplified Modification of Diet in Renal Disease (MDRD) formula based on the level of serum creatinine (SCr) :

$eGFR_{MDRD} = 186 \times$ SCr (μmol/l)$/88.4^{-1.154} \times$ age$^{-0.203} \times$ 0.742 (if female), expressed as ml/min/1.73 m^2 (Levey et al., 1999).

Statistical analysis

CysC and eGFR values were categorized into tertiles. Mean values ± standard deviations (or percentages) were calculated for all numerical variables. Differences between numerical datasets were examined by Student's *t*-test. For categorical variables, contingency tables were used to display frequency distributions. Statistical significance was calculated by Fisher's exact test. Correlations between variables were performed using the Pearson correlation test or Spearman test, as appropriate.

The correlation of CysC and eGFR with biomarkers of atherosclerosis (ICAM-1, VCAM-1, CD40L, IL-6, and TNF-α) and plaque characteristics was evaluated. Data was analysed using JMP 11 statistical software (SAS Institute, Cary, NC). A P value of < 0.05 was considered statistically significant.

Results

Basic characteristics

The range of CysC levels was 1.1–2.34 mg/l, mean 1.63 ± 0.3 mg/l, median 1.58 mg/l. The range of CysC concentrations by tertiles was as follows: tertile I, 1.1.–1.43 mg/l; tertile II, 1.44–1.64 mg/l and tertile III, 1.65–2.34 mg/l. Due to the sample size, patients in the high CysC tertile were compared to the lower tertile patients (I+II). The basic clinical characteristics and laboratory values of the study population categorized by serum CysC tertiles (III vs. I+II) are summarized in Table 1. Patients in the high CysC tertile had lower eGFR, but did not differ significantly in serum creatinine concentration.

Cystatin C and plaque magnitude

Patients in the high CysC tertile had significantly higher mean plaque burden (48.0 % ± 6.9 vs. 42.8 % ± 7.4, P = 0.029), lower mean lumen area (8.1 mm^2 ± 1.7 vs. 9.9 mm^2 ± 3.1, P = 0.044) and a higher number of 5-mm vessel segments with minimum lumen area < 4 mm^2 (17.9 ± 18.9 vs. 6.8 ± 11.7, P = 0.021) compared to patients in the lower tertiles (I+II), **(**Figs. 3-5). In addition, CysC levels demonstrated significant positive correlation with mean PB (r = 0.35, P = 0.021) and maximal PB (r = 0.3, P = 0.047).

Cystatin C and plaque composition

Neither relative, nor absolute plaque components differed significantly according to CysC tertiles. The amount of necrotic and calcified tissues was non-significantly higher (P = 0.15 and 0.24, respectively) in the high CysC tertile patients.

Table 1. Basic characteristics of study subjects according to CysC tertiles. Values are presented as mean ± standard deviation.

	Lower tertiles (N = 29)	Highest tertile (N = 15)	P
Age	63 ± 9.2	60.8 ± 9.0	0.48
Male gender	21 (72.4 %)	10 (66.7 %)	0.69
Previous MI	21 (72.4 %)	7 (46.7 %)	0.09
Family history of CAD	14 (48.3 %)	9 (60.0 %)	0.46
Arterial hypertension	25 (86.2 %)	15 (100 %)	0.06
Hyperlipidaemia	26 (89.7 %)	14 (93.3 %)	0.68
Total cholesterol (mmol/l)	4.0 ± 0.19	4.3 ± 1.1	0.42
LDL cholesterol (mmol/l)	2.2 ± 0.73	2.4 ± 0.94	0.33
HDL cholesterol (mmol/l)	1.1 ± 0.31	1.17 ± 0.46	0.57
Ejection fraction	55.6 % ± 2.8	61 % ± 1.7	0.11
Active smoking	8 (27.6 %)	5 (33.3 %)	0.69
Diabetes mellitus	6 (20.7 %)	5 (33.3 %)	0.37
Fasting glycaemia	5.7 ± 1.3	6.0 ± 1.0	0.41
Beta blockers	21 (84.2 %)	11 (73.3 %)	0.95
Statins	26 (89.7 %)	13 (86.7 %)	0.77
Calcium blockers	9 (31.0 %)	4 (26.7 %)	0.76
ACEI	23 (79.3 %)	15 (100 %)	0.06
Serum creatinine (μmol/l)	86.7 ± 16.3	78.2 ±12.5	0.06
eGFR (ml/min/1.73 m^2) MDRD	87.6 ± 13.9	72.5 ± 14.14	0.0015

Cystatin C and plaque phenotypes

The LAPS was significantly higher in the high tertile patients (0.91 ± 1.0 vs. 0.18 ± 0.92, P = 0.02) (Fig. 6). Patients in the high CysC tertile showed a trend for higher PRS compared to lower tertile subjects (3.05 ± 1.19 vs. 2.4 ± 1.1, p = 0.08). We did not observe a significant difference in plaque phenotypes between high and lower CysC tertile subjects. There was only a trend for a lower number of 5-mm vessel segments classified as "no lesion" (29.7 ± 23.9 vs. 43.7 ± 22.4, P = 0.06) and

for a higher occurrence of fibroatheromas: TCFA plus ThCFA (32.1% ± 12.7 vs. 25.4 % ± 12, P = 0.09) in the high tertile patients. However, CysC levels demonstrated a significant negative correlation with the number of "no lesion" vessel segments (r = –0.3, P = 0.048).

Cystatin C and pro-inflammatory markers

CysC levels positively, albeit modestly correlated with VCAM-1 (r = 0.37, P = 0.015) and TNF-α (r = 0.33, P = 0.027) levels (Figs. 7, 8). CysC levels did not correlate significantly with ICAM-1, CD40L and IL-6 levels.
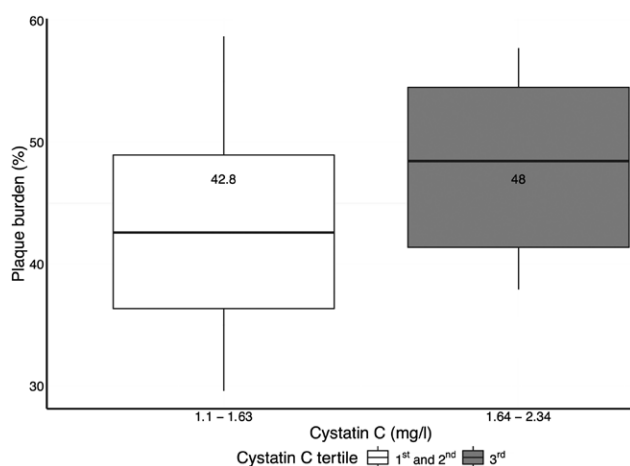

Fig. 3 Comparison of plaque burden according to CysC
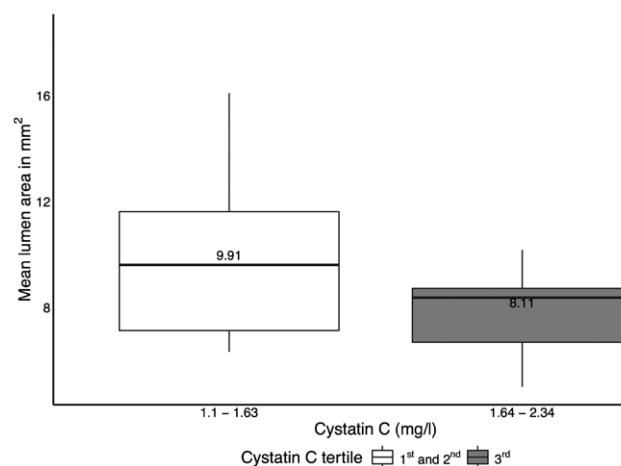The data are presented as box-plots, showing the median, 25th and 75th percentile.

Fig. 4 Comparison of mean lumen area according to CysC
The data are presented as box-plots, showing the median, 25th and 75th percentile.
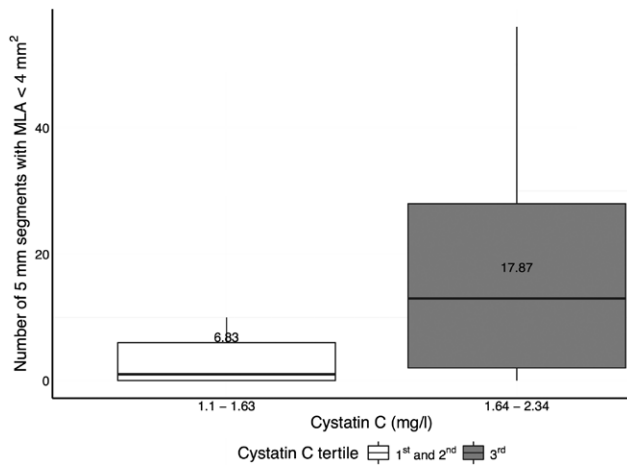
Fig. 5 Comparison of the number of 5-mm vessel segments with minimum lumen area < 4 mm^2 according to CysC tertiles
The data are presented as box-plots, showing the median, 25th and 75th percentile.
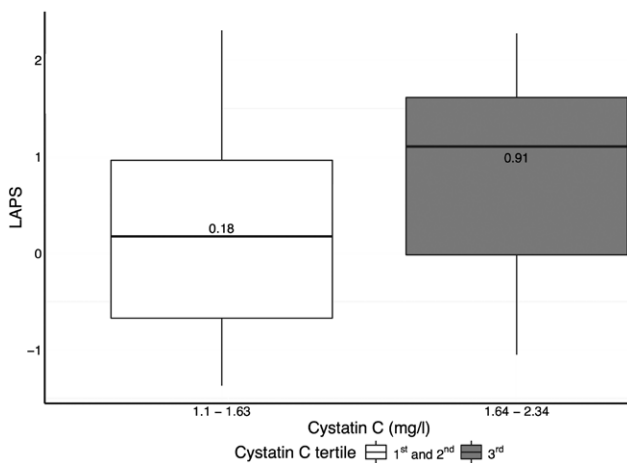

Fig. 6. Comparison of Liverpool Active Plaque Score according to CysC tertiles
The data are presented as box-plots, showing the median, 25th and 75th percentile.

eGFR and plaque characteristics

We compared patients in the low eGRF tertile with patients in the second and third eGFR tertile. We found that patients in the low eGFR tertile had:
1/ lower MLA (3.2 ± 6.4 vs. 4.4 ± 2.0, $P = 0.027$),
2/ higher maximum PB ($75.6 \% \pm 9.5$ vs. $69.5 \% \pm 9.1$, $P = 0.046$),
3/ and a higher number of 5-mm vessel segments with TCFA plaque characteristics and MLA < 4 mm^2 ($7.9 \pm 7.$ vs. 3.1 ± 5.5, $P = 0.018$).

Discussion

Previous studies have consistently shown a correlation of CysC levels with the presence and extent of coronary artery disease assessed by CAG in individuals with preserved renal function (Niccoli et al., 2008; Lee et al.,
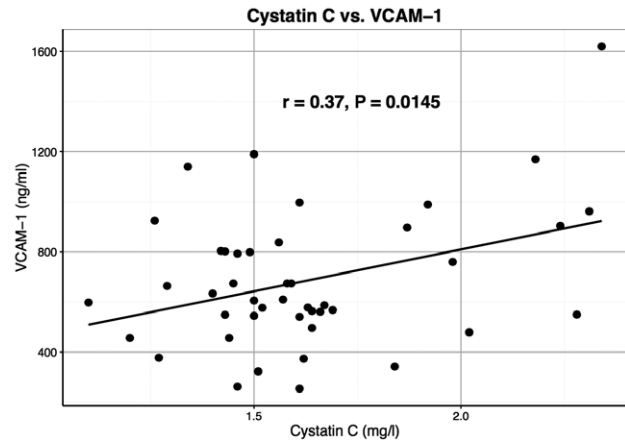

Fig. 7. Correlation between CysC and VCAM-1 levels
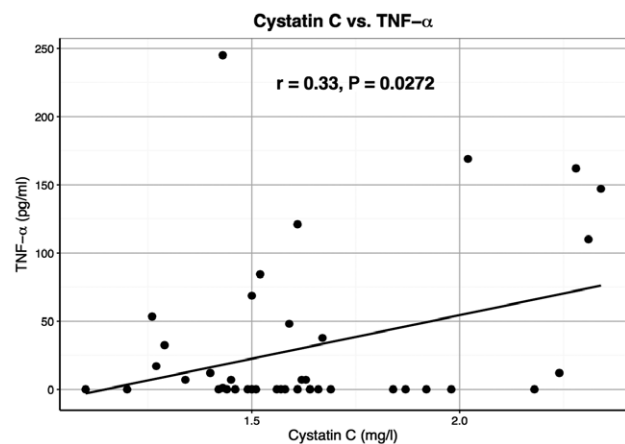Analysed by the Spearman's correlation test

Fig. 8. Correlation between CysC and TNF-α levels
Analysed by the Spearman's correlation test

2010; Wang et al., 2014). IVUS and IVUS-VH provide a much more detailed evaluation of coronary artery atherosclerosis compared to angiography including assessment of plaque magnitude, composition, and MLA, all parameters relevant to future plaque behaviour and importantly, patient outcomes (Virmani et al., 2006; Hong et al., 2007; Stone et al., 2011; Cheng et al., 2014). However, there is paucity of data on the relationship between CysC and coronary plaque morphology assessed by IVUS and IVUS-VH. Moreover, data on the relationship between CysC and plaque composition and phenotype are completely lacking.

In the present study, we demonstrated an association of CysC levels with plaque magnitude assessed by IVUS in individuals with preserved renal function, defined as eGFR > 60 ml/min/1.73 m^2. Patients with higher CysC levels had more bulky plaques expressed as higher mean plaque burden. Furthermore, we found lower mean lumen area and a higher number of vessel segments with MLA < 4 mm^2 in patients with higher CysC levels. In addition, CysC levels demonstrated a significant positive correlation with mean and maximal PB and a negative correlation with the number of "no lesion" vessel segments. Importantly, the plaque burden

has been shown to be a predictor of future cardiovascular events (Stone et al., 2011; Cheng et al., 2014). The eGFR however, was predictive neither of mean plaque burden, nor of mean lumen area. Thus, we found CysC to be a superior predictor of the total coronary atherosclerotic burden in comparison to eGRF in our cohort. Nevertheless, eGFR inversely correlated with maximal plaque burden, shown to be a risk factor for future coronary events as well (Stone et al., 2011). A study by Gu et al. (2009) found a modest positive correlation of plasma CysC with plaque area and plaque burden in patients with unstable angina, a finding in accordance with our results.

In addition to the plaque magnitude and total coronary atherosclerotic burden, the plaque composition and the presence of TCFA plaque phenotype are comparably important for further plaque evolution. A study by Hong et al. (2007) showed that patients with acute coronary syndromes have higher percentages of necrotic core and lower percentage of fibro-fatty tissue compared to patients with stable angina. In another study, Cheng et al. (2014) demonstrated that the presence of TCFAs in non-culprit coronary arteries is strongly predictive of future adverse cardiac events. In our study, both CysC and eGFR demonstrated an association with high-risk plaque characteristics. Higher CysC levels were associated with higher LAPS, a novel scoring system designed to discriminate stable and unstable coronary plaques (Murray et al., 2014). Similarly, the eGFR was associated with a higher occurrence of the TCFA plaque in conjunction with low MLA (< 4 mm^2), high risk indices shown to be significant predictors of cardiovascular events in previous large-scale studies (Calvert et al., 2011; Stone et al., 2011). Nevertheless, the absolute and relative amounts of plaque tissue components did not vary significantly according to CysC levels and eGFR in our cohort.

However, the mechanisms underlying the observed association of increased serum CysC levels with coronary artery disease remain unclear and partially speculative (Salgado et al., 2013; Wang et al., 2014). Likewise, the extent to which the levels of circulating CysC are determined by mechanisms other than GFR remains only partly elucidated (Stevens et al., 2006; Taglieri et al., 2009). Moreover, the discrepancy between consistently documented increased serum CysC levels in individuals with more advanced atherosclerosis and decreased CysC levels in atherosclerotic plaques remains unresolved (Shi et al., 1999; Koc et al., 2010; Wang et al., 2014). Several hypotheses striving to elucidate the link of increased serum CysC levels to atherosclerosis have emerged in the past years. Firstly, CysC is perceived as a sensitive marker of impaired renal function, which represents an established cardiovascular risk factor (Go et al., 2004). Abundant data indicate that even mild renal impairment is associated with a pro-inflammatory state, increased oxidative stress, lipoprotein abnormalities and pertubations in vascular wall lipid trafficking, leading to accelerated atherosclerosis (de Boer et al., 2008; Wang et al., 2008; Zuo et al., 2009; Nerpin et al., 2012). However, many researchers have linked CysC with cardiovascular disease and events within normal ranges of GFR (Lee et al., 2010; Salgado et al., 2013). Moreover, cardiovascular risk associated with higher CysC levels was found to be eGFR independent in several studies (Ix et al., 2007; Patel et al., 2013).

Secondly, elevated CysC has been related to a pro-inflammatory state characterized by increased hs-CRP and fibrinogen levels (Urbonaviciene et al., 2011; Wang et al., 2014). Some authors speculate that higher serum CysC concentrations could result from increased CysC production by cytokine-stimulated cell lines during the atherosclerotic process, thus presumably compensating for the decreased tissue levels of CysC and increased cathepsin-related proteolytic activity in atherosclerotic plaques (Taglieri et al., 2009; Salgado et al., 2013).

We have demonstrated a positive correlation of CysC with VCAM-1 and TNF-α levels. On the other hand, CysC did not correlate with ICAM-1, IL-6, and CD40L levels. IL-6, an important pro-inflammatory cytokine, may contribute to plaque instability by promoting the expression of MMPs and TNF-α (Zakynthinos and Pappa, 2009). Several studies suggested IL-6 levels to be predictive of adverse cardiac events; however, the utility of IL-6 as a biomarker is weakened by its substantial circadian variation and lacking confirmatory studies (Zakynthinos and Pappa, 2009). Soluble CD40L is a pro-inflammatory marker involved crucially in plaque destabilization and atherothrombosis. Not surprisingly, CD40L was predictive of adverse cardiovascular events in many studies (Zakynthinos and Pappa, 2009; Zhang et al., 2013). Cell adhesion molecules, e.g. VCAM-1 and ICAM-1, play a principal role in the interactions between leucocytes, thrombocytes and endothelial cells, i.e. in the early steps of atherosclerosis (Nakashima et al., 1998). Elevated VCAM-1 levels were predictive of future cardiovascular events in patients after an acute coronary syndrome (Mulvihill et al., 2001) as well as in the general CAD population (Blankenberg et al., 2001). In contrast, ICAM-1 was not a predictor of cardiovascular events in both patient populations (Blankenberg et al., 2001; Mulvihill et al., 2001). In our previous study, VCAM-1 was a significant predictor of coronary artery plaque burden (Kovarnik et al., 2013). Thus, VCAM-1 appears to correlate intimately with both the coronary artery disease burden and cardiovascular events. TNF-α is perceived as one of the principal mediators of endothelial dysfunction and atherogenesis (Kleinbogard et al., 2010), and elevated TNF-α levels are predictive of recurrent coronary events after myocardial infarction (Ridker et al., 2000).

In summary, our findings support the notion that chronic inflammation, characterized by increased VCAM-1 and TNF-α levels, contributes to the association of higher serum CysC levels with more advanced coronary atherosclerosis in individuals with preserved renal function according to eGFR. Our data suggest that serum CysC represents a sensitive biomarker of mild renal dysfunc-

tion not unmasked by eGFR, and presumably of chronic inflammation, processes leading to the development of more advanced coronary atherosclerosis.

Furthermore, the genetically determined variation of CysC levels has been evaluated in relation to atherosclerosis in several studies. The *CysC* gene is regarded as a housekeeping gene, indicating stable production of CysC by most cellular types (Salgado et al., 2013). However, studies on the association of *CysC* gene variants affecting serum CysC concentrations with atherosclerosis have reported conflicting results (Eriksson et al., 2004; Loew et al., 2005; Svensson-Färbom et al., 2015). Thus, the genetically determined variation of serum CysC levels does not seem to be related to altered risk of atherosclerosis (Svensson-Färbom et al., 2015).

In conclusion, our study demonstrated a significant association of increased CysC levels with more advanced coronary artery disease characterized by more bulky plaques, lower mean lumen area and higher risk plaque phenotype in patients with preserved renal function. Moreover, CysC was found to be a superior predictor of risk plaque features, compared to eGFR. Our observations support the hypothesis that CysC does not merely represent an early marker of renal insufficiency, and that additional mechanisms may be involved in the association of increased CysC levels with more advanced coronary atherosclerosis. Given our findings and the prognostic significance of CysC in patients with coronary artery disease demonstrated in other studies, we suggest to incorporate CysC measurement into the risk stratification algorithm of these patients. Larger-scale trials are warranted to confirm and further extend our preliminary findings.

References

Bengtsson, E., To, F., Håkansson, K., Grubb, A., Brånén, L., Nilsson, J., Jovinge, S. (2005). Lack of the cysteine protease inhibitor cystatin C promotes atherosclerosis in apolipoprotein E-deficient mice. *Arterioscler. Thromb. Vasc. Biol.* **25**, 2151-2156.

Blankenberg, S., Rupprecht, H. J., Bickel, C., Peetz, D., Hafner, G., Tiret, L., Meyer, J. (2001) Circulating cell adhesion molecules and death in patients with coronary artery disease. *Circulation* **104**, 1336-1342.

de Boer, I. H., Astor, B. C., Kramer, H., Palmas, W., Seliger, S. L., Shlipak, M. G., Siscovick, D. S., Tsai, M. Y., Kestenbaum, B. (2008) Lipoprotein abnormalities associated with mild impairment of kidney function in the multi-ethnic study of atherosclerosis. *Clin. J. Am. Soc. Nephrol.* **3**, 125-132.

Calvert, P. A., Obaid, D. R., O'Sullivan, M., Shapiro, L. M., McNab, D., Densem, C. G., Schofield, P. M., Braganza, D., Clarke, S. C., Ray, K. K., West, N. E., Bennett, M. R. (2011) Association between IVUS findings and adverse outcomes in patients with coronary artery disease: the VIVA (VH-IVUS in Vulnerable Atherosclerosis) Study. *JACC Cardiovasc. Imaging* **4**, 894-901.

Cheng, J. M., Garcia-Garcia, H. M., de Boer, S. P., Kardys, I., Heo, J. H., Akkerhuis, K. M., Oemrawsingh, R. M., van Domburg, R. T., Ligthart, J., Witberg, K. T., Regar, E., Serruys, P. W., van Geuns, R. J., Boersma, E. (2014) In vivo detection of high-risk coronary plaques by radiofrequency intravascular ultrasound and cardiovascular outcome: results of the ATHEROREMO-IVUS study. *Eur. Heart J.* **35**, 639-647.

Cheng, X. W., Huang, Z., Kuzuya, M., Okumura, K., Murohara, T. (2011) Cysteine protease cathepsins in atherosclerosis-based vascular disease and its complications. *Hypertension* **58**, 978-986.

Eriksson, P., Deguchi, H., Samnegård, A., Lundman, P., Boquist, S., Tornvall, P., Ericsson, C. G., Bergstrand, L., Hansson, L. O., Ye, S., Hamsten, A. (2004) Human evidence that the cystatin C gene is implicated in focal progression of coronary artery disease. *Arterioscler. Thromb. Vasc. Biol.* **24**, 551-557.

Frendéus, K. H., Wallin, H., Janciauskiene, S., Abrahamson M. (2009) Macrophage responses to interferon-γ are dependent on cystatin C levels. *Int. J. Biochem. Cell Biol.* **41**, 2262-2269.

Garcia-Garcia, H. M., Mintz, G. S., Lerman, A., Vince, D. G., Margolis, M. P., van Es, G. A., Morel, M. A., Nair, A., Virmani, R., Burke, A. P., Stone, G. W., Serruys, P. W. (2009) Tissue characterisation using intravascular radiofrequency data analysis: recommendations for acquisition, analysis, interpretation and reporting. *EuroIntervention* **5**, 177-189.

Go, A. S., Chertow, G. M., Fan, D., McCulloch, C. E., Hsu, C. Y. (2004) Chronic kidney disease and the risks of death, cardiovascular events, and hospitalization. *N. Engl. J. Med.* **351**, 1296-1305.

Gu, F. F., Lü, S. Z., Chen, Y. D., Zhou, Y. J., Song, X. T., Jin, Z. N., Liu, H. (2009) Relationship between plasma cathepsin S and cystatin C levels and coronary plaque morphology of mild to moderate lesions: an in vivo study using intravascular ultrasound. *Chin. Med. J.* **122**, 2820-2826.

Hong, M. K., Mintz, G. S., Lee, C. W., Suh, J., Kim, J. H., Park, D. W., Lee S. W., Kim, Y. H., Cheong, S. S., Kim, J. J., Park, S. W., Park, S. J. (2007) Comparison of virtual histology to intravascular ultrasound of culprit coronary lesions in acute coronary syndrome and target coronary lesions in stable angina pectoris. *Am. J. Cardiol.* **100**, 953-959.

Hong, Y. J., Jeong, M. H., Choi, Y. H., Park, S. Y., Rhew, S. H., Jeong, H. C., Cho, J. Y., Jang, S. Y., Lee, K. H., Park, K. H., Sim, D. S., Yoon, N. S., Yoon, H. J., Kim, K. H., Park, H. W., Kim, J. H., Ahn, Y., Cho, J. G., Park, J. C., Kang, J. C. (2013) Comparison of coronary plaque components between non-culprit lesions in patients with acute coronary syndrome and target lesions in patients with stable angina: virtual histology-intravascular ultrasound analysis. *Korean Circ. J.* **43**, 607-614.

Ix, J. H., Shlipak, M. G., Chertow, G. M., Whooley, M. A. (2007) Association of cystatin C with mortality, cardiovascular events, and incident heart failure among persons with coronary heart disease: data from the Heart and Soul Study. *Circulation* 115, 173-179.

Kiyosue, A., Hirata, Y., Ando, J., Fujita, H., Morita, T., Takahashi, M., Nagata, D., Kohro, T., Imai, Y., Nagai, R. (2010) Plasma cystatin C concentration reflects the severity of coronary artery disease in patients without chronic kidney disease. *Circ. J.* **74**, 2441-2447.

Kleinbongard, P., Heusch, G., Schulz, R. (2010) TNF-α in atherosclerosis, myocardial ischemia/reperfusion and heart failure. *Pharmacol. Ther*. **127**, 295-314.

Koc, M., Batur, M. K., Karaarslan, O., Abali, G. (2010) Clinical utility of serum cystatin C in predicting coronary artery disease. *Cardiol. J*. **17**, 374-380.

Kovarnik, T., Kral, A., Skalicka, H., Mintz, G. S., Kralik, L., Chval, M., Horak, J., Skalicka, L., Sonka, M., Wahle, A., Downe, R. W., Uhrova, J., Benakova, H., Cernohousova, L., Martasek, P., Belohlavek, J., Aschermann, M., Linhart, A. (2013) The prediction of coronary artery disease based on non-invasive examinations and heme oxygenase 1 polymorphism versus virtual histology. *J. Invasive Cardiol*. **25**, 32-37.

Lee, M., Saver, J. L., Huang, W. H., Chow, J., Chang, K. H., Ovbiagele, B. (2010) Impact of elevated cystatin C level on cardiovascular disease risk in predominantly high cardiovascular risk populations: a meta-analysis. *Circ. Cardiovasc. Qual. Outcomes* **3**, 675-683.

Levey, A. S., Bosch, J. P., Lewis, J. B., Greene, T., Rogers, N., Roth, D. (1999) A more accurate method to estimate glomerular filtration rate from serum creatinine: a new prediction equation. Modification of Diet in Renal Disease Study Group. *Ann. Intern. Med*. **130**, 461-470.

Li, K., Wu, X., Chen, D. Z., Sonka, M. (2006) Optimal surface segmentation in volumetric images – a graph-theoretic approach. *IEEE Trans. Pattern Anal. Mach. Intell*. **28**, 119-134.

Loew, M., Hoffmann, M. M., Koenig, W., Brenner, H., Rothenbacher, D. (2005) Genotype and plasma concentration of cystatin C in patients with coronary heart disease and risk for secondary cardiovascular events. *Arterioscler. Thromb. Vasc. Biol*. **25**, 1470-1474.

Mintz, G. S., Nissen, S. E., Anderson, W. D., Bailey, S. R., Erbel, R., Fitzgerald, P. J., Pinto, F. J., Rosenfield, K., Siegel, R. J., Tuzcu, E. M., Yock, P. G. (2001) American College of Cardiology clinical expert consensus document on standards for acquisition, measurement and reporting of intravascular ultrasound studies (IVUS). A report of the American College of Cardiology Task Force on Clinical Expert Consensus Documents. *J. Am. Coll. Cardiol*. **37**, 1478-1492.

Mintz, G. S., Garcia-Garcia, H. M., Nicholls, S. J., Weissman, N. J., Bruining, N., Crowe, T., Tardif, J. C., Serruys, P. W. (2011) Clinical expert consensus document on standards for acquisition, measurement and reporting of intravascular ultrasound regression/progression studies. *EuroIntervention* **6**, 1123-1130.

Mulvihill, N. T., Foley, J. B., Murphy, R. T., Curtin, R., Crean, P. A., Walsh, M. (2001) Risk stratification in unstable angina and non-Q wave myocardial infarction using soluble cell adhesion molecules. *Heart* **85**, 623-627.

Murray, S. W., Stables, R. H., Garcia-Garcia, H. M., Grayson, A. D., Shaw, M. A., Perry, R. A., Serruys, P. W., Palmer, N. D. (2014) Construction and validation of a plaque discrimination score from the anatomical and histological differences in coronary atherosclerosis: the Liverpool IVUS-V-HEART (Intra Vascular UltraSound-Virtual-Histology Evaluation of Atherosclerosis Requiring Treatment) study. *EuroIntervention* **10**, 815-823.

Nair, A., Kuban, B. D., Tuzcu, M., Schoenhagen, P., Nissen, S. E., Vince, D. G. (2002) Coronary plaque classification with intravascular ultrasound radiofrequency data analysis. *Circulation* **106**, 2200-2206.

Nakashima, Y., Raines, E., Plump, A., Breslow, J. L., Ross, R. (1998) Upregulation of VCAM-1 and ICAM-1 at atherosclerosis-prone sites on the endothelium in the ApoE-deficient mouse. *Arterioscler. Thromb. Vasc. Biol*. **18**, 842-851.

Nerpin, E., Helmersson-Karlqvist, J., Risérus, U., Sundström, J., Larsson, A., Jobs, E., Basu, S., Ingelsson, E., Arnlöv, J. (2012) Inflammation, oxidative stress, glomerular filtration rate, and albuminuria in elderly men: a cross-sectional study. *BMC Res. Notes* **5**, 537.

Niccoli, G., Conte, M., Della Bona, R., Altamura, L., Siviglia, M., Dato, I., Ferrante, G., Leone, A. M., Porto, I., Burzotta, F., Brugaletta, S., Biasucci, L. M., Crea, F. (2008) Cystatin C is associated with an increased coronary atherosclerotic burden and a stable plaque phenotype in patients with ischemic heart disease and normal glomerular filtration rate. *Atherosclerosis* **198**, 373-380.

Patel, D., Ahmad, S., Silverman, A., Lindsay, J. (2013) Effect of cystatin C levels on angiographic atherosclerosis progression and events among postmenopausal women with angiographically decompensated coronary artery disease (from the Women's Angiographic Vitamin and Estrogen [WAVE] study). *Am. J. Cardiol*. **111**, 1681-1687.

Ridker, P., Rifai, N., Pfeffer, M., Sacks, F., Lepage, S., Braunwald, E. (2000) Elevation of tumor necrosis factor-α and increased risk of coronary events after myocardial infarction. *Circulation* **101**, 2149-2153.

Sai, E., Shimada, K., Miyauchi, K., Masaki,Y., Kojima, T., Miyazaki, T., Kurata, T., Ogita, M., Tsuboi, S., Yoshihara, T., Miyazaki, T., Ohsaka, A., Daida, H. (2016) Increased cystatin C levels as a risk factor of cardiovascular events in patients with preserved estimated glomerular filtration rate after elective percutaneous coronary intervention with drug-eluting stents. *Heart Vessels* **31**, 694-701.

Salgado, J. V., Souza, F. L., Salgado, B. J. (2013) How to understand the association between cystatin C levels and cardiovascular disease: imbalance, counterbalance, or consequence? *J. Cardiol*. **62**, 331-335.

Shi, G. P., Sukhova, G. K., Grubb, A., Ducharme, A., Rhode, L. H., Lee, R. T., Ridker, P. M., Libby, P., Chapman, H. (1999) Cystatin C deficiency in human atherosclerosis and aortic aneurysm. *J. Clin. Invest*. **104**, 1191-1197.

Shlipak, M. G., Sarnak, M. J., Katz, R., Fried, L. F., Seliger, S. L., Newman, A. B., Siscovick, D. S., Stehman-Breen, C. (2005) Cystatin C and the risk of death and cardiovascular events among elderly persons. *N. Engl. J. Med*. **352**, 2049-2060.

Silva, D., Cortez-Dias, N., Jorge, C., Marques, J. S., Carrilho-Ferreira, P., Magalhães, A., Martins, S. R., Gonçalves, S., da Silva, P. C., Fiúza, M., Diogo, A. N., Pinto, F. J. (2012) Cystatin C as prognostic biomarker in ST-segment elevation acute myocardial infarction. *Am. J. Cardiol*. **109**, 1431-1438.

Stevens, L.A., Coresh, J., Greene, T., Levey, A. S. (2006) Assessing kidney function-measured and estimated glomerular filtration rate. *N. Engl. J. Med*. **354**, 2473-83.

Stone, G. W., Maehara, A., Lansky, A., de Bruyne, B., Cristea, E., Mintz, G. S., Mehran, R., McPherson, J., Farhat, N., Marso, S. P., Parise, H., Templin, B., White, R., Zhang, Z., Serruys, P. W. (2011) A prospective natural-history study of coronary atherosclerosis. *N. Engl. J. Med.* **364**, 226-235.

Sun, S., Sonka, M., Beichel, R. R. (2013) Graph-based IVUS segmentation with efficient computer-aided refinement. *IEEE Trans. Med. Imaging* **32**, 1536-1549.

Sukhova, G. K., Shi, G. P., Simon, D. I., Chapman, H. A., Libby, P. (1998) Expression of the elastolytic cathepsins S and K in human atheroma and regulation of their production in smooth muscle cells. *J. Clin. Invest.* 102, 576-583.

Sukhova, G. K., Wang, B., Libby, P., Pan, J. H., Zhang, Y., Grubb, A., Fang, K., Chapman, H. A., Shi, G. P. (2005) Cystatin C deficiency increases elastic lamina degradation and aortic dilatation in apolipoprotein E-null mice. *Circ. Res.* 96, 368-375.

Svensson-Färbom, P., Almgren, P., Hedblad, B., Engström, G., Persson, M., Christensson, A., Melander, O. (2015) Cystatin C is not causally related to coronary artery disease. *PLoS One* **10**, e0129269.

Taglieri, N., Koenig, W., Kaski, J. C. (2009) Cystatin C and cardiovascular risk. *Clin. Chem.* 55, 1932-1943.

Urbonaviciene, G., Shi, G. P., Urbonavicius, S., Henneberg, E. W., Lindholt, J. S. (2011) Higher cystatin C level predicts long-term mortality in patients with peripheral arterial disease. *Atherosclerosis* **216**, 440-445.

Verdot, L., Lalmanach, G., Vercruysse, V., Hoebeke J., Gauthier, F., Vray, B. (1999) Chicken cystatin stimulates nitric oxide release from interferon-γ activated mouse peritoneal macrophages via cytokine synthesis. *Eur. J. Biochem.* **266**, 1111-1117.

Virmani, R., Burke, A. P., Farb, A., Kolodgie, F. D. (2006) Pathology of the vulnerable plaque. *J. Am. Coll. Cardiol.* **47**, C13-18.

Wahle, A., Prause, P. M., DeJong, S. C., Sonka, M. (1999) Geometrically correct 3D reconstruction of intravascular ultrasound images by fusion with biplane angiography – methods and validation. *IEEE Trans. Med. Imaging* **18**, 686-699.

Wahle, A., Lopez, J. J., Olszewski, M. E., Vigmostad, S. C., Chandran, K. B., Rossen, J. D., Sonka, M. (2006) Plaque development, vessel curvature, and wall shear stress in coronary arteries assessed by X-ray angiography and intravascular ultrasound. *Med. Image Anal.* **10**, 615-631.

Wang, J., Sim, A. S., Wang, X. L., Salonikas, C., Moriatis, M., Naidoo, D., Wilcken, D. E. (2008) Relations between markers of renal function, coronary risk factors and the occurrence and severity of coronary artery disease. *Atherosclerosis* **197**, 853-859.

Wang, G. N., Sun, K., Hu, D. L., Wu, H. H., Wang, X. Z., Zhang, J. S. (2014) Serum cystatin C levels are associated with coronary artery disease and its severity. *Clin. Biochem.* **47**, 176-181.

Xu, Y., Ding, Y., Li, X., Wu, X. (2015) Cystatin C is a disease associated protein subject to multiple regulation. *Immunol. Cell. Biol.* **93**, 442-451.

Yin, Y., Zhang, X., Williams, R., Wu, X., Anderson, D. D., Sonka, M. (2010) LOGISMOS – layered optimal graph image segmentation of multiple objects and surfaces: cartilage segmentation in the knee joint. *IEEE Trans. Med. Imaging* **29**, 2023-2037.

Zakynthinos, E., Pappa, N. (2009) Inflammatory biomarkers in coronary artery disease. *J. Cardiol.* **53**, 317-333.

Zhang, B., Wu, T., Chen, M., Zhou, Y., Yi, D., Guo, R. (2013) The CD40/CD40L system: a new therapeutic target for disease. *Immunol. Lett.* **153**, 58-61.

Zuo, Y., Yancey, P., Castro, I. Khan, W. N., Motojima, M., Ichikawa, I., Fogo, A. B., Linton, M. F., Fazio, S., Kon, V. (2009) Renal dysfunction potentiates foam cell formation by repressing ABCA1. *Arterioscler. Thromb. Vasc. Biol.* **29**, 1277-1282.